

Bridgman grown $\text{Hg}_{1-x}\text{Cd}_x\text{Te}$: crystalline quality assessment by X-ray topography

A. B. TRIGUBO, I. NOLLMANN*, J. R. CASANOVA†

*Comision Nacional de Investigaciones Cientificas y Tecnicas, *Comision Nacional de Investigaciones Espaciales and †Instituto de Investigaciones Cientificas y Tecnicas de las Fuerzas Armadas, CITEFA-DINSO, Zufriategui 4380, 1603 Villa Martelli, Provincia de Buenos Aires, Argentina*

Different growth speeds and thermal annealings were applied to Bridgman grown crystals. Several characterization methods (X-ray topography, energy dispersive atomic spectroscopy (EDAX) etc.) showed that the most suitable conditions are a high growing speed and a thermal treatment of no less than 30 days.

1. Introduction

$\text{Hg}_{1-x}\text{Cd}_x\text{Te}$ (MCT) is a semiconductor alloy of narrow band gap energy. Infrared detectors usable in the second atmospheric window at 77 K can be obtained for $x = 0.2$. For high purity material, grain and subgrain boundaries have adverse electrical effects on detectors [1, 2], so high quality single crystals must be obtained to improve the performance of the detectors. Bridgman [3] and CRA [4] (cast, recrystallization, annealing) growth methods have been applied to get the material. Both can be considered as solidification from the melting techniques. The phase diagram [5] determines a compositional dispersion (Δx) along the growth axis [6] of the ingots. Crystalline quality is decreased with higher growth speed in the Bridgman method [5]; meanwhile, compositional dispersion Δx diminishes [5]. Subsequent thermal annealings can improve both parameters.

In this paper we compare different growth speeds and subsequent thermal treatments of the ingots aiming to decrease the Δx dispersion and to increase the grain and subgrain size. An electron beam microprobe was employed to determine the x composition, meanwhile X-rays studies have been used to evaluate crystalline quality. Even when the purity of the starting elements was not adequate to obtain opto-electronic grade material, it was decided to start with the growth studies in order to determine the influence of the different factors affecting the crystalline quality. Hall effect measurements [7] were used to study the electrical properties.

2. Experimental procedure

99.9999% purity elements (Hg, Cd, Te) were employed to obtain $x = 0.2$ MCT; a Hg excess was used to compensate the free volume of the ampoule [8].

Growth speed values of 1–96 cm day^{-1} (Table I) were used to obtain ingots 1–4 by the conventional Bridgman method [9]. CRA method ($v =$

7200 cm day^{-1}) was used to get ingot 5, which can be considered as a Bridgman growth technique with a very high growing speed value [5]. The ingots were 7 mm in diameter and roughly 50 mm in length. Ingots 3–5 received a subsequent thermal annealing in the growth ampoule to increase the grain size and decrease the compositional dispersion.

The wafers were obtained by perpendicular cuts to the growth axis, except in ingot 2 where the cut was performed along the axis. The usual mechanical and chemical polishing procedures were applied [10]. An electron beam microprobe EDAX allowed us to determine the x composition of the ingots with 10% precision. Laue X-ray diagrams were used to determine crystalline orientation [11] and CuK_α X-ray topography (reflection Lang's method) [12–14] was employed for the crystalline characterization. The beam divergence was 3' except ingot 4 in which 15' was used also.

3. Results and discussion

3.1. Composition

Fig. 1 shows the x -Cd composition of the different ingots, its dispersion Δx is shown in Table II. It can be observed large Δx dispersion values were obtained with low growth speed (1 and 2.4 cm day^{-1}). In agreement with previously published results [5] it can be seen clearly (Fig. 2) that the composition dispersion, Δx , decreases when the growth speed increases. The lower Δx value of ingot 4, compared to ingot 3 can be attributed to the beneficial effect of the subsequent long time thermal treatment (30 days).

3.2. Crystalline quality

3.2.1. Ingot orientation

Laue diffraction diagrams performed on wafers belonging to ingots 1–4 showed that single crystals from 1.5–5 cm in length could be found along the growth axis, with a maximum of three grains in each ingot [15, 16]. There is no preferential orientation of these

TABLE I Grown ingots

Ingot number <i>N</i>	Growth speed <i>v</i> (cm day ⁻¹)	Thermal gradient (C cm ⁻¹)	Remarks	Subsequent ingot thermal treatment	
				<i>T</i> (°C)	<i>t</i> (days)
1	1	40	No excess Hg was used	—	—
2	2.4	40	Excess Hg was used	—	—
3	96	45	to compensate	610	10
4	96	45	the free volume	650	30 ^a
5	7200	—	of the ampoule	650	10

^a Long time thermal treatment

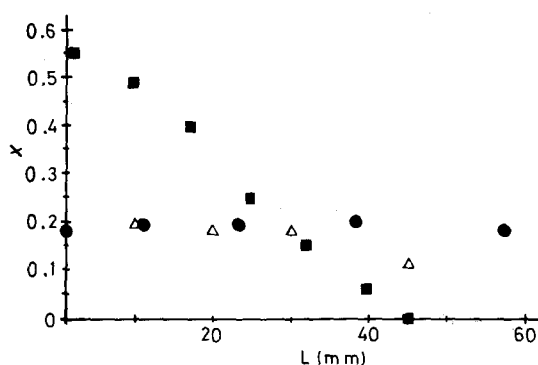


Figure 1 Longitudinal ingot composition: (■) ingot 2; (Δ) ingot 4; (●) ingot 5.

TABLE II Ingots dispersion composition

Ingot number <i>N</i>	Growth speed, <i>v</i> (cm day ⁻¹)	Cd composition range	Composition dispersion Δx
1	1	$0 < x < 0.55$	0.55
2	2.4	$0 < x < 0.55$	0.55
3	96	$0.14 < x < 0.26$	0.12
4	96	$0.11 < x < 0.19$	0.08 ^a
5	7200	$0.18 < x < 0.20$	0.02

^a Long time thermal treatment

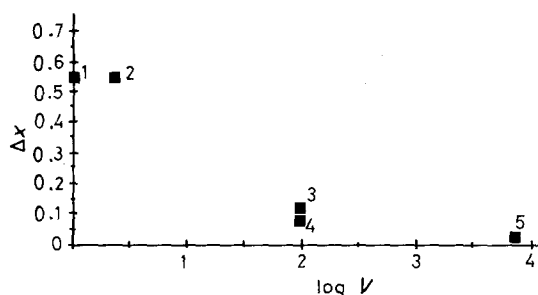


Figure 2 Δx values of the ingots grown in different speed conditions. The ingot number is shown in the graph.

grains with respect to the ingot axis and a large misorientation can exist between them.

Ingot 5 (CRA) has several grains with a high misorientation between them in each wafer. No X-ray topography studies could be performed on this sample because of the small area of each grain [17].

3.2.2. X-ray topography

Four topographies ($g = 444$) were obtained from a wafer of ingot 1 varying the angle of incidence in 200' steps (Fig. 3). This procedure was used in order to determine the subgrain structure and to obtain the size of the low misorientation areas in all the studied wafers.

For a total angular variation $\Delta\phi = 600''$ of the incidence angle, the size of the equal orientation crystalline zone was determined (Table III) through the value of the percentual iso-orientated area parameter ($A\%$) that makes it possible to compare results obtained from samples with dispersion in the surface area. It is defined by

$$A\% = \frac{\text{Total reflected area for } \Delta\phi}{\text{Total sample area}} \times 100$$

In this case the $A\%$ value is 55. A homogeneous subgrain structure with polygonal contours and a typical area of 0.1 mm² (Table III) can be observed by contrast orientation [14]. A heat treatment of 7 days at $T = 300^\circ\text{C}$ of the sample did not change its grain or subgrain structure.

Ingot 2 was cut along the growing axis to study the granular structure in this direction. One half of it was studied as-grown and the other was submitted to a heat treatment of 10 days at 500 °C. Studies similar to those performed on ingot 1 did not show any change due to the heat treatment. Fig. 4 and Table III include the results obtained for the sample thermally treated. It showed a columnar subgrain structure with a typical subgrain area of 0.1 mm².

Topographs obtained from two samples of ingot 3 confirm, as could be expected, that the grain size and the value of $A\%$ decrease when the growing speed is increased. A micrograph of the studies performed on the sample is shown (Fig. 5, Table III). The values of the typical subgrain area and the $A\%$ of ingot 3 show that even with the subsequent thermal treatment applied ($T = 610^\circ\text{C}$, $t = 10$ days) there is a significant decrease in the crystalline quality with increasing growth speed.

On the other side, a set of topographies from a wafer of ingot 4, which had received a subsequent thermal treatment of 30 days at 650 °C show that its typical subgrain area is comparable to that of ingot 1, although a higher subgrain area dispersion exists (Fig. 6a, Table III). The $A\%$ value of 70 obtained after the heat treatment is remarkable, in fact it is even higher

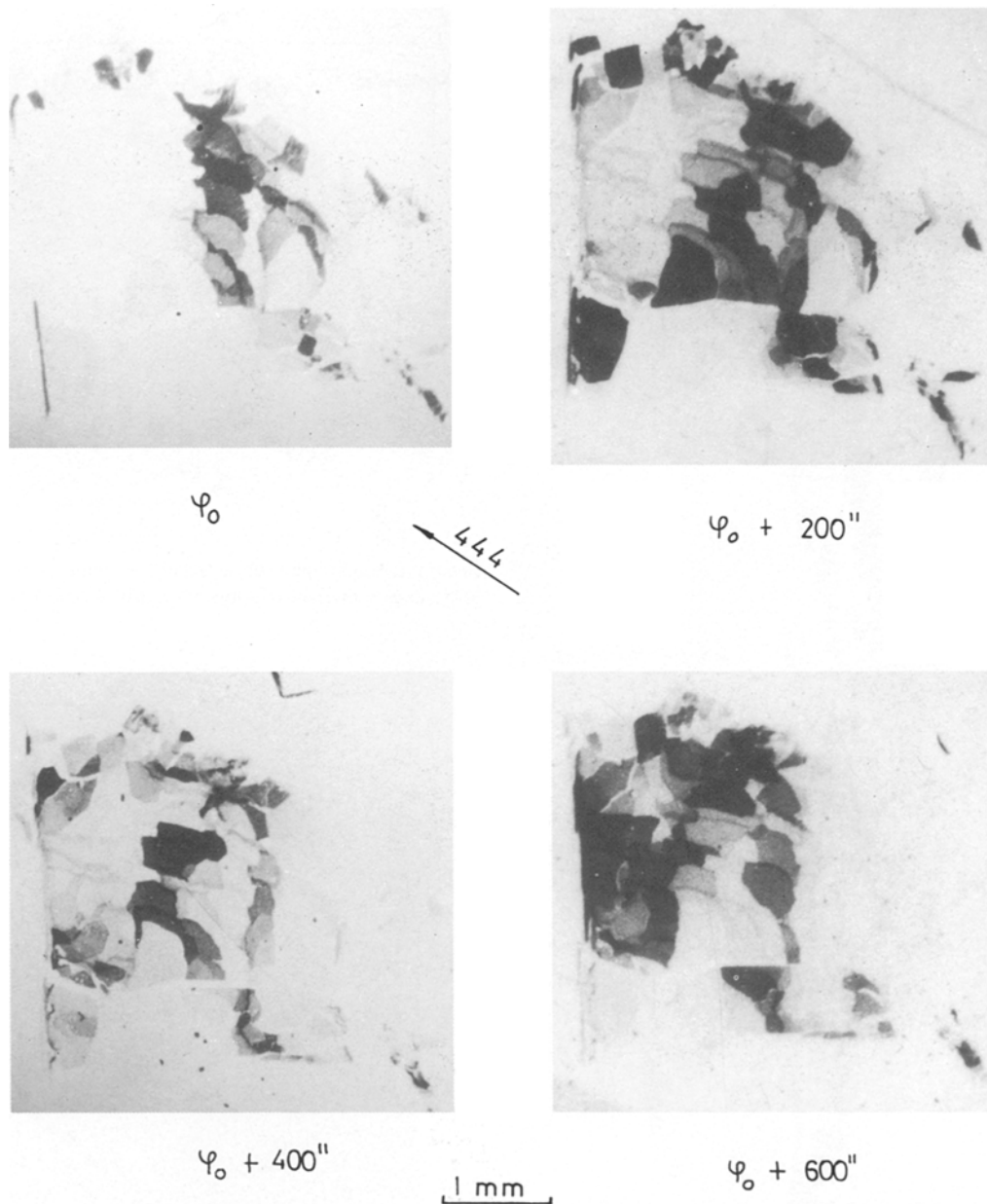


Figure 3 Set of topographies of a wafer of ingot 1—growth speed: 1 cm day^{-1} ; thermal treatment: $T = 300^\circ\text{C}$, $t = 7$ days.

TABLE III Representative crystalline parameters

Ingot number N	v (cm day^{-1})	$A\%$ (a), (b)	Typical subgrain area, a (mm^2) (b)	Remarks
1	1	55	0.1	The heat treatment applied to the sample did not show effect on the crystalline structure
2	2.4	longitudinal cut	0.1	
3	96	20	0.02	Time or temperature of the heat treatment were too short or low, respectively.
4	96	70	0.07	Adequate thermal treatment
5	7200	Too small	Too small	No topographies were obtained because of the small value of $A\%$.

^a $\Delta\varphi \sim 10'$ min

^b Estimated errors: $\frac{\Delta A\%}{A\%} \sim 0.1$; $\frac{\Delta a}{a} \sim 0.2$

than the $A\%$ value of ingot 1, which had been grown at 1 cm day^{-1} . This result shows the important influence of the heat treatments over the grain and subgrain structure of Bridgman grown MCT. Moreover,

taking the total misorientation of the grain ($33'$) the $A\%$ value results, 92, means that nearly the whole area has the same orientation.

Fig. 6b shows a topography of the above mentioned

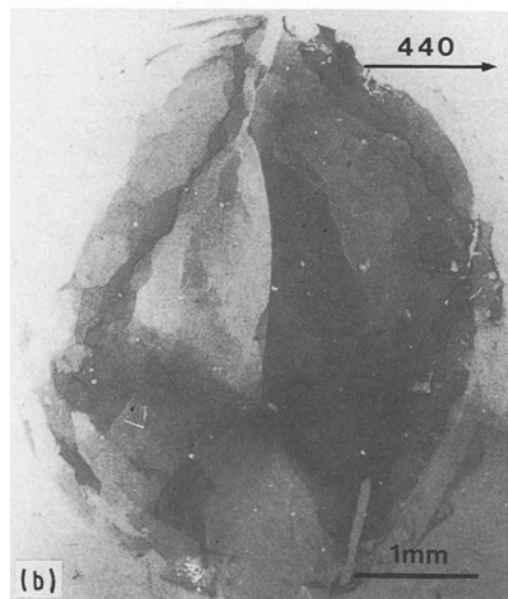
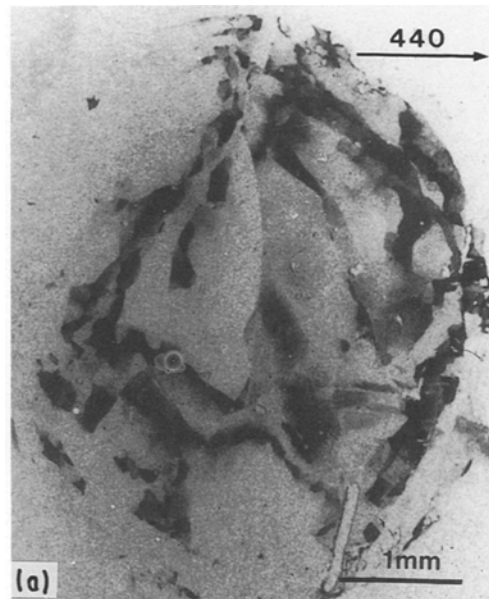
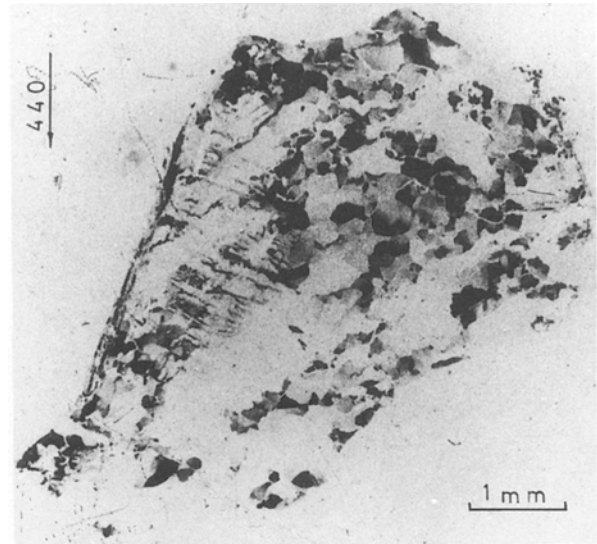


Figure 4 Topography of a wafer of ingot 2—growth speed: 2.4 cm day^{-1} ; thermal treatment: $T = 500^\circ\text{C}$, $t = 10$ days.

wafer taken with a beam angular divergence of $15'$; it gives a general vision of the latter. Chemical etching studies done over this wafer and another one of the same ingot cut at 1 cm of the previous one, showed a complete correspondance of the subgrain structure [18], revealing the existence of a large grain formed by an arrangement of subgrains of columnar structure, as it was observed in ingot 2 (Fig. 4).

3.3. Electrical characterization

Hall effect measurements [7] have been obtained by the Van der Paw method (19, 20). At 77 K , carrier

Figure 6 Topography of a wafer of ingot 4—growth speed: 96 cm day^{-1} ; thermal treatment: $T = 650^\circ\text{C}$, $t = 30$ days: (a) 3 min beam divergence, (b) 15 min beam divergence.

concentration of 10^{16} – 10^{17} cm^{-3} and Hall mobilities of 10^3 – 10^4 $\text{cm}^2 \text{V}^{-1} \text{s}^{-1}$ were obtained in most samples. No correlation between these values and the composition x or crystalline quality could be found because any effect is masked by the impurity level, as we previously supposed based on the fact that 99.9999% purity is not adequate to obtain intrinsic material ($n_i \sim 10^{14}$ cm^{-3} at 77 K). Hall effect measurements confirm that the high impurity density determines the majority carrier concentration type and value and limited their Hall mobility.

4. Conclusions

From the present studies we can conclude that even with low purity material (99.9999%) it is possible to obtain good crystalline quality and low composition dispersion MCT single crystals provided that the appropriate values of growth speed, and subsequent heat treatment temperatures and times are chosen.

Acknowledgements

The authors thank E. Heredia for the Hall effect measurements and to G. Padula for her assistance in the photographic laboratory.

References

1. H. F. MATARE, "Defect Electronics in Semiconductors", (Wiley-Interscience, USA, 1971) p. 145.
2. D. J. WILLIAMS and A. W. VERE, *J. Crystal Growth* **83** (1987) 341.
3. B. E. BARLETT, J. DEANS and P. C. ELLEN, *J. Mater. Sci.* **4** (1969) 266.
4. K. L. BYE, *ibid.* **14** (1979) 619.
5. W. F. H. MICKLETHWAITE, in "Semiconductors and Semimetals", edited by R. K. Willardson and A. C. Beer (Academic Press, 1981) p. 47.
6. D. LONG and J. L. SCHMIT, *ibid.* (Academic Press, 1970) p. 175.
7. E. HEREDIA, M. BIANCHETTI, C. FREZZOTTI and R. D'ELIA, AFA Conference, Rosario, Argentina, October 1985 (AFA Press).
8. G. DITTMAR, *Krist. Tech.* **12** (1977) 631.
9. M. BIANCHETTI, R. D'ELIA, C. FREZZOTTI, G. MAHR von STASZEWSKI, I. NOLLMANN, A. B. TRIGUBO and N. E. WALSOE de RECA, *Rev. Teleg. Electr.* **6** (1985) 177.
10. E. L. POLISAR, N. M. BOJNYK, G. V. INDENBAUM, A. V. VANYUKOV and V. P. SCHASTHIVYI, *J. Sov. Phys.* **11** (1968) 48.
11. B. D. CULLITY, in "Elements of X-ray diffraction", (Addison-Wesley, 1959) p. 215.
12. B. K. TANNER, in "X-ray diffraction topography" (Pergamon Press 1976) p. 28.
13. E. S. MEIERAN, *Siemens Review*, **XXXVII** (1970) 39.
14. A. R. LANG, in "Modern diffraction and imaging techniques in materials science", edited by S. Amelinckx, R. Gevers, G. Remaut and J. Van Landuyt (Elsevier, 1970) p. 407.
15. J. R. CASANOVA, E. HEREDIA, A. N. NORDIN and A. B. TRIGUBO, AFA Conference, Bariloche, Argentina, October 1987 (AFA Press).
16. J. R. CASANOVA, E. HEREDIA, I. NOLLMANN and A. B. TRIGUBO, AFA Conference, Mar del Plata, Argentina, October 1988 (AFA Press).
17. J. R. CASANOVA, I. NOLLMANN, G. MAHR von STASZEWSKI, A. B. TRIGUBO and N. E. WALSOE de RECA, in Proceedings of the Second Brazilian School of Semiconductor Physics II February (University of Sao Paulo Press, 1985) p. 1029.
18. I. NOLLMAN, A. B. TRIGUBO and N. E. WALSOE de RECA, Proceedings of the X Inter-American Conference on Materials Technology, San Antonio, Texas, USA, April 1989 (Southwest Research Inst Press) pp. 30–1.
19. L. J. VAN DER PAW, *Philips Tech. Rev.* **20** (1958) 220.
20. *Idem*, *Philips Res. Repts.* **13** (1958) 1.

Received 16 August 1990
and accepted 28 February 1991